Journal of Alloys and Compounds 509 (2011) 9034–9037

Contents lists available at ScienceDirect

Journal of Alloys and Compounds

journal homepage: www.elsevier.com/locate/jallcom

Glass forming ability and crystallization of Zr–Cu–Ag–Al–Be bulk metallic glasses

F. Xu, H.B. Lou, X.D. Wang*, S.Q. Ding, Q.P. Cao, J.Z. Jiang*

International Center for New-Structured Materials (ICNSM), Zhejiang University and Laboratory of New-Structured Materials, Department of Materials Science and Engineering, Zhejiang University, Hangzhou 310027, PR China

ARTICLE INFO

Article history:
Received 25 December 2010
Received in revised form 17 February 2011
Accepted 19 February 2011
Available online 26 February 2011

Keywords:
Bulk metallic glass
Glass forming ability
Crystallization
Be addition

ABSTRACT

The glass forming ability of $Zr_{46}Cu_{37.64-x}Ag_{8.36}Al_8Be_x$ (x = 0, 6 and 10 at.%) bulk metallic glasses (BMGs) were significantly improved by Be addition. The critical size of amorphous rods can be over 35 mm diameter. The high GFA achieved is mainly due to the decrease of melting point and liquidus temperature, and suppression of the formation of crystalline phases during solidification from liquid state. The high stabilization with supercooled liquid regime of 115 K was found for the BMG with x = 10 at.%. Two independent exothermic events happen in x = 0 and 6 at.% BMGs, corresponding to the formation of primary crystalline phases $Cu_{10}Zr_7$ and AgZr, then transforming to final stable crystalline phases Zr_2Cu and $AlCu_2Zr$. However, in the x = 10 at.% BMG, the precipitation of primary phases and transformation to final stable phases are within the first exothermic event and the $AlCu_2Zr$ phase is totally suppressed.

1. Introduction

Glass forming ability and crystallization of bulk metallic glasses (BMGs) are important issues [1–18]. The crystallization of BMGs is accompanied by significant changes in many properties. This imposes a strict limit on the operating times at elevated temperatures for such advanced engineering materials. With the development of multicomponent systems, the critical size of BMGs has been greatly improved, providing good prototypes to study their inherent nature of crystallization behaviors. Recently, a new class of Zr–Cu–Ag–Al BMGs was developed [19–21], for which the maximum size can be over 20 mm in diameter by copper mold casting. It is known that minor alloying can be an effective method to further improve the glass forming ability (GFA) [22]. In this work, by minor addition of a fifth element to the Zr–Cu–Ag–Al BMGs system, its GFA is successfully improved above 35 mm in diameter by copper mold casting. The crystallization behaviors of three representative BMGs are investigated by X-ray diffraction (XRD) and differential scanning calorimeter (DSC) in detail. The correlation of the structural difference with GFA is discussed.

2. Experimental methods

Pre-alloyed ingots with nominal compositions $Zr_{46}Cu_{37.64}Ag_{8.36}Al_8$, $Zr_{46}Cu_{31.64}Ag_{8.36}Al_8Be_6$, $Zr_{46}Cu_{27.64}Ag_{8.36}Al_8Be_{10}$ were prepared by arc melting high purity (>99.9%) Cu, Zr, Ag and Al with commercial CuBe alloy in a Ti-gettered purified argon atmosphere. The compositions were designed just by tuning the atomic ratio between Cu and CuBe alloy. 10, 20 and 35 mm diameter rods were prepared by copper mold casting under argon atmosphere after the ingots were remelted in an Al_2O_3 crucible by induction in a home-made high vacuum (4×10^{-3} Pa) casting equipment. The amorphous nature of as-cast samples up to 35 mm in diameter was ascertained by X-ray diffractometer (Philips X'Pert) measurements with Cu Kα radiation and a differential scanning calorimeter (Netzsch DSC 404c). The thin pieces were cut from 10 mm diameter as-cast rods and heated to the selected temperatures in DSC. The annealed samples were then cooled down to ambient temperature and polished to remove the surface oxide layer. Possible crystalline phases in the annealed samples were examined by XRD. For crystalline phase identification software Jade was used [23]. The volume fractions of the precipitated crystalline component in annealed samples were roughly evaluated by calculating the peak area in exothermic events on their DSC traces during reheating annealed samples to 1273 K.

3. Results and discussion

Fig. 1 shows the XRD patterns taken from the central region in the transverse cross section of three as-cast bulk cylinder samples with 35 mm diameter prepared by copper mold casting. Sharp Bragg peaks appear on the pattern of the $Zr_{46}Cu_{37.64}Ag_{8.36}Al_8$ sample, indicating that the sample is not amorphous but crystalline. The major precipitate crystalline phase is $Cu_{10}Zr_7$ phase, possibly together with minor Zr_2Cu and $AlCu_2Zr$ phases. However, XRD patterns display only broad diffraction maxima for $Zr_{46}Cu_{31.64}Ag_{8.36}Al_8Be_6$ and $Zr_{46}Cu_{27.64}Ag_{8.36}Al_8Be_{10}$, representing the characteristic feature of an amorphous structure. Thus, the GFA of $Zr_{46}Cu_{37.64}Ag_{8.36}Al_8$ sample that formerly was reported as 20 mm in diameter can be improved to at least 35 mm by minor Be addition. Fig. 2 shows the DSC traces for these three samples in 10 mm diameter measured at a heating rate of 20 K/min. The characteristic temperatures and GFA parameters: supercooled liquid regime $\Delta T_x = T_x - T_g$ [24], reduced glass transition temperature

* Corresponding authors.
E-mail addresses: wangxd@zju.edu.cn (X.D. Wang), jiangjz@zju.edu.cn (J.Z. Jiang).

0925-8388/$ – see front matter © 2011 Published by Elsevier B.V.
doi:10.1016/j.jallcom.2011.02.107

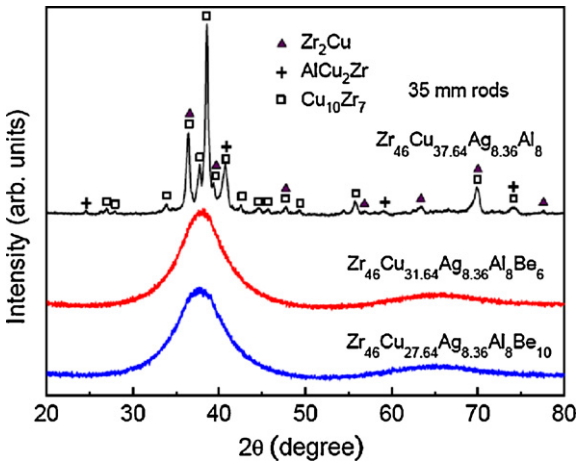

Fig. 1. XRD patterns taken from the central region in the transverse cross section of three as-cast bulk cylinder samples with 35 mm diameter prepared by copper mold casting.

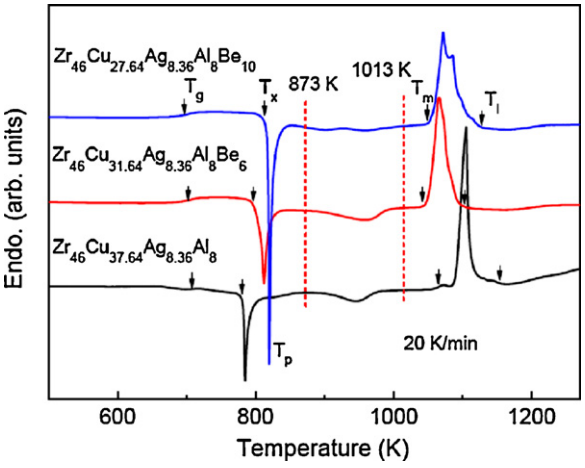

Fig. 2. DSC traces for three amorphous samples with a heating rate of 20 K/min, in which characteristic temperatures and selected heating temperatures, T_p (peak temperature in the first exothermic event), 873 K and 1013 K are labeled.

$T_{rg} = T_g/T_l$ [25] and gamma factor $\gamma = T_x/(T_g + T_l)$ [26] are listed in Table 1. The enhanced GFA can be present by increased ΔT_x, T_{rg} and γ values since Be addition not only increases the onset crystallization temperature T_x but also reduces the melting point T_m and liquidus temperature T_l. The highest T_{rg} value of 0.636 for $Zr_{46}Cu_{31.64}Ag_{8.36}Al_8Be_6$ suggests that this alloy could have the higher GFA.

To study crystallization behaviors of these three samples, thin slices were cut from 10 mm diameter amorphous rods and heated in DSC furnace to three selected temperatures, T_p (peak temperature of the first exothermic event), 823 K (after the first exothermic event) and 1013 K (after the second) as shown in Fig. 2. Without holding time at the selected temperature, the sample was cooled to room temperature subsequently. The effect of this pre-annealing treatment could be reflected in the following DSC traces

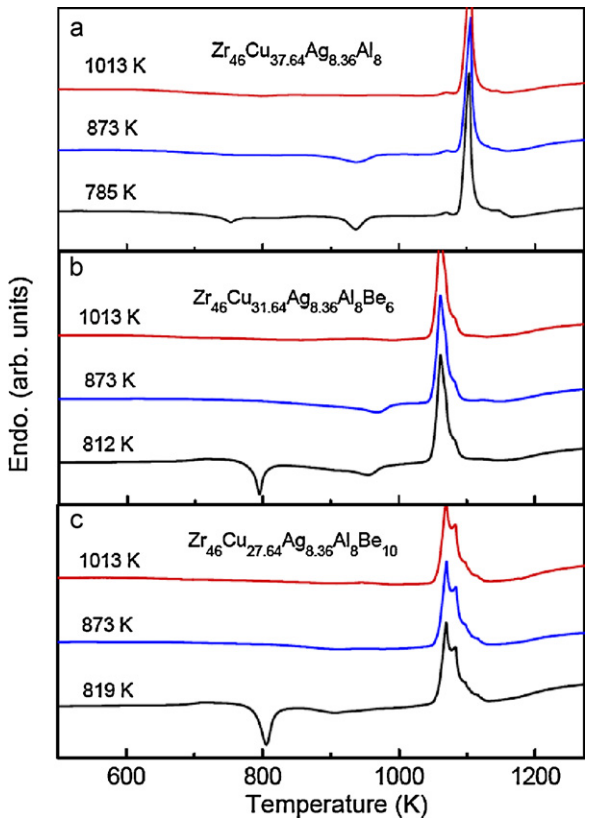

Fig. 3. DSC traces measured for three samples after cooled down to room temperature from the selected heating temperatures.

as shown in Fig. 3. It is demonstrated that the material undergoes crystallization in a controlled but not a reversible manner. For $Zr_{46}Cu_{37.64}Ag_{8.36}Al_8$ and $Zr_{46}Cu_{31.64}Ag_{8.36}Al_8Be_6$ BMGs, two exothermic events exist and for $Zr_{46}Cu_{27.64}Ag_{8.36}Al_8Be_{10}$ only one appears, indicating different crystallization behaviors between them. In order to determine different crystallization behaviors exactly, XRD measurements for samples after annealing treatments at various selected temperatures were carried out. Fig. 4 illustrates the crystallization behaviors of these three BMGs. All identified crystalline phases are listed in Table 2. For $Zr_{46}Cu_{37.64}Ag_{8.36}Al_8$ BMG, the major primary crystalline phase detected is $Cu_{10}Zr_7$ together with a minor AgZr phase appearing at 785 K. When annealing temperature increases to 873 K, the major crystalline phases are still $Cu_{10}Zr_7$ and AgZr. However, after the second exothermic event, phase transformations to Zr_2Cu and $AlCu_2Zr$ are detected in the sample annealed at 1013 K. XRD patterns for $Zr_{46}Cu_{31.64}Ag_{8.36}Al_8Be_6$ BMG show that it experiences almost the same events in the $Zr_{46}Cu_{37.64}Ag_{8.36}Al_8$ BMG upon heating at low temperatures. However, at 1013 K the fraction of $AlCu_2Zr$ phase largely decreases and some other unknown crystalline phases are detected. For the $Zr_{46}Cu_{27.64}Ag_{8.36}Al_8Be_{10}$ BMG annealed at 798 K, the same $Cu_{10}Zr_7$ phase with minor AgZr phase were detected as primary crystalline phases while crystalline phases are almost the same for the samples annealed at 873 K and 1013 K. This is consis-

Table 1
Characteristic temperatures (glass transition temperature T_g, onset crystallization temperature T_x, melting point T_m and liquidus temperature T_l) and glass-forming-ability parameters (supercooled liquid regime $\Delta T_x = T_x - T_g$, reduced glass transition temperature $T_{rg} = T_g/T_l$ and gamma factor $\gamma = T_x/(T_g + T_l)$) for $Zr_{46}Cu_{37.64}Ag_{8.36}Al_8$, $Zr_{46}Cu_{31.64}Ag_{8.36}Al_8Be_6$ and $Zr_{46}Cu_{27.64}Ag_{8.36}Al_8Be_{10}$ BMGs.

Samples	T_g (K)	T_x (K)	T_m (K)	T_l (K)	ΔT_x (K)	T_{rg}	γ
$Zr_{46}Cu_{37.64}Ag_{8.36}Al_8$	707	780	1064	1154	73	0.613	0.419
$Zr_{46}Cu_{31.64}Ag_{8.36}Al_8Be_6$	702	797	1042	1103	95	0.636	0.442
$Zr_{46}Cu_{27.64}Ag_{8.36}Al_8Be_{10}$	697	813	1050	1129	115	0.617	0.445

Table 2
Possible crystalline phases detected in the annealed $Zr_{46}Cu_{37.64}Ag_{8.36}Al_8$, $Zr_{46}Cu_{31.64}Ag_{8.36}Al_8Be_6$ and $Zr_{46}Cu_{27.64}Ag_{8.36}Al_8Be_{10}$ samples.

Samples	T_p	873 K	1013 K
$Zr_{46}Cu_{37.64}Ag_{8.36}Al_8$	$Cu_{10}Zr_7$ + AgZr	$Cu_{10}Zr_7$ + AgZr	Zr_2Cu + $AlCu_2Zr$
$Zr_{46}Cu_{31.64}Ag_{8.36}Al_8Be_6$	$Cu_{10}Zr_7$ + AgZr	$Cu_{10}Zr_7$ + AgZr	Zr_2Cu + $AlCu_2Zr$ + unknown
$Zr_{46}Cu_{27.64}Ag_{8.36}Al_8Be_{10}$	$Cu_{10}Zr_7$ + AgZr	Zr_2Cu + $Cu_{10}Zr_7$ + unknown	Zr_2Cu + unknown

tent with DSC data in Fig. 2 without the second exothermic event. It should be stressed that the $AlCu_2Zr$ phase, which is detected in other two samples annealed at high temperature, is not detected in this $Zr_{46}Cu_{27.64}Ag_{8.36}Al_8Be_{10}$ BMG annealed at high temperatures. Here, we could conclude that in these three BMGs, $Cu_{10}Zr_7$ phase appears mainly in the primary phase. With increasing of Be content to 10 at.%, $AlCu_2Zr$ phase is gradually suppressed in the final crystalline products. This indicates that high GFA obtained by adding the fifth element of Be in the Zr–Cu–Ag–Al system could be linked with the suppression of the formation of crystalline $AlCu_2Zr$ phase during solidification process from liquid state.

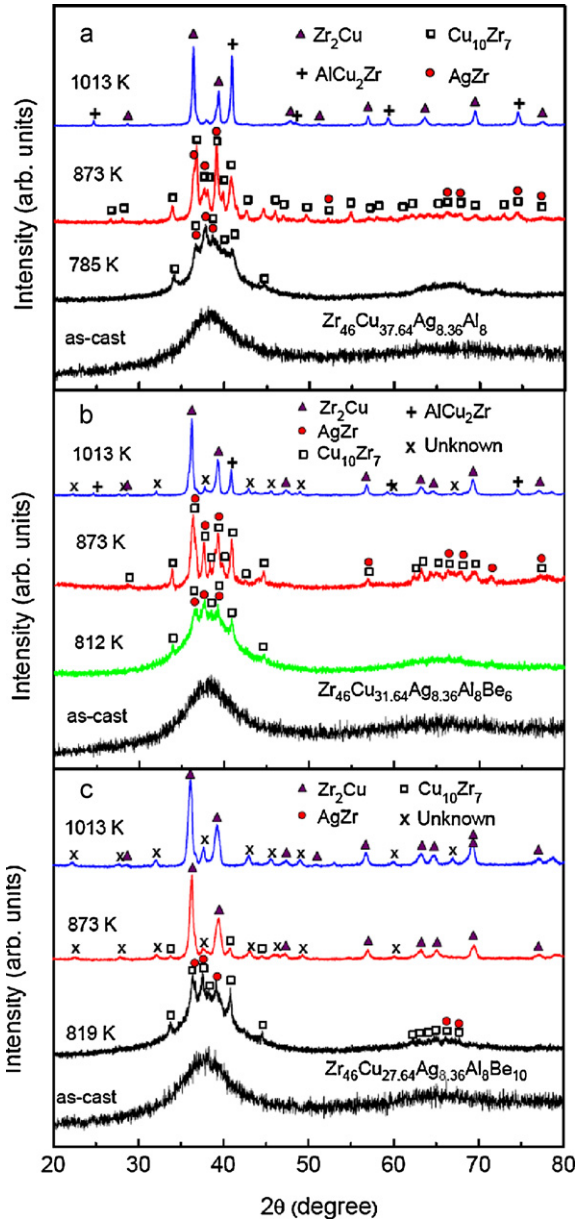

Fig. 4. XRD patterns for three samples (10 mm diameter) in the as-cast and pre-annealed states, respectively.

Atomic radius of Be is about 1.13 Å, which is smaller than Cu (1.28 Å), Zr (1.60 Å), Ag (1.44 Å), and Al (1.43 Å). Thus, introducing Be into Zr–Cu–Ag–Al system could make the atomic packing much denser (density differences between crystalline and amorphous states for the same composition alloy experimentally determined are 0.681% for $Zr_{46}Cu_{37.64}Ag_{8.36}Al_8$, 0.586% for $Zr_{46}Cu_{31.64}Ag_{8.36}Al_8Be_6$, and 0.437% for $Zr_{46}Cu_{27.64}Ag_{8.36}Al_8Be_{10}$, respectively), and suppress the movement of atoms. This is proved by the fact that the onset crystallization temperature is increased with Be content, i.e., 780 K for Be = 0 at.%, 797 K for Be = 6 at.% and 813 K for Be = 10 at.%, creating the largest supercooled liquid regime of 115 K for $Zr_{46}Cu_{27.64}Ag_{8.36}Al_8Be_{10}$ BMG. On the other hand, the lowest melting point and liquidus temperature were achieved in $Zr_{46}Cu_{31.64}Ag_{8.36}Al_8Be_6$ BMG. It is commonly believed that to shorten the temperature regime between T_l and T_g is the most important factor for glass formation [27]. Thus, the reduced liquidus temperature and high stabilized liquid phase are the major characteristics of strong glass formers. The melting point of Be is about 1560 K, higher than that of Cu 1356.6 K, Ag 1235.1 K and Al 933.5 K. The decreased melting point of $Zr_{46}Cu_{31.64}Ag_{8.36}Al_8Be_6$ alloy is possibly due to the composition closer to the eutectic point. Forming a homogeneous eutectic structure [28] in a limited experimental time scale could be suppressed upon rapid cooling, causing an enhanced GFA of $Zr_{46}Cu_{31.64}Ag_{8.36}Al_8Be_6$ BMG.

4. Conclusions

It is found that Be addition can significantly improve the glass forming ability of Zr–Cu–Ag–Al BMG, making the critical size over 35 mm in diameter. The high GFA achieved is mainly due to the melting point and liquidus temperature decrease. Also, Be addition can promote the atomic packing density, and increase the stabilization of the amorphous phase by suppressing the formation of crystalline phases during heating. The primary phases of $Zr_{46}Cu_{37.64}Ag_{8.36}Al_8$ and $Zr_{46}Cu_{31.64}Ag_{8.36}Al_8Be_6$ BMGs are $Cu_{10}Zr_7$ and AgZr while the final stable phases are mainly Zr_2Cu and $AlCu_2Zr$. However, in $Zr_{46}Cu_{27.64}Ag_{8.36}Al_8Be_{10}$ BMG, $AlCu_2Zr$ phase is totally suppressed and primary phases could transform to final stable phases within the first exothermic event in a transient mode.

Acknowledgement

Financial supports from the National Natural Science Foundation of China (grant nos. 51071141, 50920105101, 51050110136, 10979002, 60876002, 50890174, 10804096 and 10904127), Qianjiang Program, Zhejiang University-Helmholtz cooperation fund, and the Department of Science and Technology of Zhejiang province are gratefully acknowledged.

References

[1] A. Inoue, T. Zhang, T. Masumoto, Mater. Trans. JIM 31 (1990) 177.
[2] A. Gebert, J. Eckert, L. Schultz, Acta Mater. 46 (1998) 5475.
[3] R. Busch, S. Schneider, A. Peker, W.L. Johnson, Appl. Phys. Lett. 67 (1995) 1544.
[4] L.Q. Xing, J. Eckert, W. Löser, L. Schultz, D.M. Herlach, Philos. Mag. A 79 (1999) 1095.
[5] X.D. Wang, H.S. Lee, S. Yi, Mater. Lett. 60 (2006) 935.
[6] X.D. Wang, Q. Wang, J.Z. Jiang, J. Alloys Compd. 440 (2007) 189.

[7] Q.K. Jiang, G.Q. Zhang, L.Y. Chen, Q.S. Zeng, J.Z. Jiang, J. Alloys Compd. 242 (2006) 179.
[8] Q.K. Jiang, G.Q. Zhang, L.Y. Chen, J.Z. Wu, H.G. Zhang, J.Z. Jiang, J. Alloys Compd. 242 (2006) 183.
[9] Q.K. Jiang, X.P. Nie, Y.G. Li, Y. Jin, Z.Y. Chang, X.M. Huang, J.Z. Jiang, J. Alloys Compd. 443 (2007) 191.
[10] F. Xu, Y.L. Du, P. Gao, Z.D. Han, G. Chen, S.Q. Wang, J.Z. Jiang, J. Alloys Compd. 441 (2007) 76.
[11] F. Xu, Z.M. Wang, Z.R. Yuan, G. Chen, J.Z. Jiang, J. Alloys Compd. 458 (2008) 261.
[12] X. Ou, G.Q. Zhang, X. Xu, L.N. Wang, J.F. Liu, J.Z. Jiang, J. Alloys Compd. 441 (2007) 181.
[13] X. Ou, W. Roseker, K. Saksl, H. Franz, L. Gerward, X. Xu, G.Q. Zhang, L.N. Wang, J.F. Liu, J.Z. Jiang, J. Alloys Compd. 441 (2007) 185.
[14] H.T. Hu, L.Y. Chen, X.D. Wang, Q.P. Cao, J.Z. Jiang, J. Alloys Compd. 460 (2008) 714.
[15] X.M. Huang, C.T. Chang, Z.Y. Chang, X.D. Wang, Q.P. Cao, B.L. Shen, A. Inoue, J.Z. Jiang, J. Alloys Compd. 460 (2008) 708.
[16] X.M. Huang, X.D. Wang, J.Z. Jiang, J. Alloys Compd. 485 (2009) L35.
[17] M. Stefan, K. Saksl, P. Svovic, J.Z. Jiang, J. Alloys Compd. 478 (2009) 441.
[18] J. Bednarcik, C. Curfs, M. Sikorski, H. Franz, J.Z. Jiang, J. Alloys Compd. 504 (2010) S155.
[19] G.Q. Zhang, Q.K. Jiang, L.Y. Chen, M. Shao, J.F. Liu, J.Z. Jiang, J. Alloys Compd. 242 (2006) 176.
[20] Q.K. Jiang, X.D. Wang, X.P. Nie, G.Q. Zhang, H. Ma, H.J. Fecht, J. Bednarcik, H. Franz, Y.G. Liu, Q.P. Cao, J.Z. Jiang, Acta Mater. 56 (2008) 1785.
[21] W. Zhang, Q.S. Zhang, A. Inoue, J. Mater. Res. 23 (2008) 1452.
[22] W.H. Wang, Prog. Mater. Sci. 52 (2007) 540.
[23] Materials Data Inc., http://www.materialsdata.com/, JADE 5, XRD Pattern Processing.
[24] T. Zhang, A. Inoue, T. Masumoto, Mater. Trans. JIM 32 (1991) 1005.
[25] D. Turnbull, Contemp. Phys. 10 (1969) 473.
[26] Z.P. Lu, C.T. Liu, Acta Mater. 50 (2002) 3501.
[27] J.H. Perepezko, J.S. Smith, J. Non-Cryst. Solids 44 (1981) 65.
[28] D. Ma, H. Tan, Y. Li, Acta Mater. 53 (2005) 2969.